

Revisiting Metastable Dark Energy and Tensions in the Estimation of Cosmological Parameters

XIAOLEI LI,^{1,2,3} ARMAN SHAFIELOO,^{2,4} VARUN SAHNI,⁵ AND ALEXEI A. STAROBINSKY^{6,7}

¹*Department of Physics, Hebei Normal University, Shijiazhuang 050024, China*

²*Korea Astronomy and Space Science Institute, Daejeon 34055, Korea*

³*Quantum Universe Center, Korean Institute of Advanced Studies, Hoegiro 87, Dongdaemun-gu, Seoul 130-722, Korea*

⁴*University of Science and Technology, Yuseong-gu 217 Gajeong-ro, Daejeon 34113, Korea*

⁵*Inter-University Centre for Astronomy and Astrophysics, Pune, India*

⁶*L. D. Landau Institute for Theoretical Physics, Moscow 119334, Russia*

⁷*National Research University Higher School of Economics, Moscow 101000, Russia*

(Dated: November 28, 2019)

ABSTRACT

We investigate constraints on some key cosmological parameters by confronting metastable dark energy models with different combinations of the most recent cosmological observations. Along with the standard Λ CDM model, two phenomenological metastable dark energy models are considered: (i) DE decays exponentially, (ii) DE decays into dark matter. We find that: (1) when considering the most recent supernovae and BAO data, and assuming a fiducial Λ CDM model, the inconsistency in the estimated value of the $\Omega_{m,0}h^2$ parameter obtained by either including or excluding Planck CMB data becomes very much substantial and points to a clear tension (Sahni et al. 2014; Zhao et al. 2017); (2) although the two metastable dark energy models that we study provide greater flexibility in fitting the data, and they indeed fit the SNe Ia+BAO data substantially better than Λ CDM, they are not able to alleviate this tension significantly when CMB data are included; (3) while local measurements of the Hubble constant are significantly higher relative to the estimated value of H_0 in our models (obtained by fitting to SNe Ia and BAO data), the situation seems to be rather complicated with hints of inconsistency among different observational data sets (CMB, SNe Ia+BAO and local H_0 measurements). Our results indicate that we might not be able to remove the current tensions among different cosmological observations by considering simple modifications of the standard model or by introducing minimal dark energy models. A complicated form of expansion history, different systematics in different data and/or a non-conventional model of the early Universe might be responsible for these tensions.

Keywords: Cosmology: observational - Dark Energy - Methods: statistical

1. INTRODUCTION

The nature of Dark energy (DE) is a key open issue in modern cosmology. The presence of DE may be required to explain an accelerating universe as suggested by observations of Type Ia Supernovae (SNe Ia) (Riess et al. 1998; Perlmutter et al. 1999), and supported by measurements of large scale structure (LSS) and the cosmic microwave background radiation (CMB) (Spergel et al. 2003; Abazajian et al. 2004; Tegmark et al. 2004; Eisen-

stein et al. 2005; Komatsu et al. 2009). The simplest and best known candidate for dark energy is the cosmological constant Λ whose value remains unchanged as the Universe expands. While current observational data are in agreement with the standard Λ CDM cosmology, General Relativity (GR) with a cosmological constant, though being completely consistent intrinsically at the classical level and having no more problems than GR itself at the quantum level, faces some well-known theoretical difficulties, such as the “fine-tuning” and “cosmic coincidence” problems, when trying to relate the observed small and positive value of the cosmological constant to parameters of the Standard Model of elementary parti-

cles and its generalizations like the string theory (Sahni & Starobinsky 2000; Bean et al. 2005). Recent papers have also drawn attention to some other difficulties faced by Λ CDM including tension between the value of H_0 estimated by fitting to the acoustic peaks in the *Planck* CMB power spectrum (Collaboration et al. 2014; Ade et al. 2016; Aghanim et al. 2018) and that obtained from distance scale estimates (Sahni et al. 2014; Ding et al. 2015; Zheng et al. 2016; Solà et al. 2017; Alam et al. 2017b; Shanks et al. 2018). In order to alleviate these problems, different solutions such as dark energy models beyond Λ CDM model, modifications to general relativity theory and other physically-motivated possibilities like modifications to the dark matter sector have been put forward (Ko et al. 2017; Raveri et al. 2017; Kumar & Nunes 2017; Di Valentino et al. 2017; Renk et al. 2017; Solà et al. 2017; Di Valentino et al. 2018; Khosravi et al. 2019; Poulin et al. 2019; Vattis et al. 2019; Li & Shafieloo 2019; Pan et al. 2019).

A new class of ‘Metastable DE’ models was introduced in Shafieloo et al. (2017). In these models DE decays into other dark sector components of the Universe such as dark matter or dark radiation. The rate of decay of DE depends only upon its ‘intrinsic’ properties and not on extrinsic considerations such as the rate of expansion of the universe, etc. The metastable DE model was largely inspired by the radioactive decay of heavy nuclei into lighter elements. A total of three metastable DE models were considered, namely, i) DE decays exponentially, ii) DE decays into non-baryonic Dark Matter (DM), iii) DE decays into Dark Radiation. We should note that from a theoretical perspective one can achieve metastable behaviour of dark energy from an intermediate phase of quantum vacuum decay (Szydlowski et al. 2017, 2018). It was found that model II showed less tension between CMB and QSO based $H(2.34)$ BAO data than that faced by Λ CDM. Clearly in order to understand DE, one has to turn to cosmological observations. In previous work, DE models have been discussed in the context of different kinds of cosmological observations (Cao et al. 2015; Li et al. 2016; Zheng et al. 2017; Shafieloo et al. 2017; Li et al. 2017). For metastable DE models, Shafieloo et al. (2017) used 580 SNe Ia from the Union-2.1 compilation (Suzuki et al. 2012) and four BAO data sets in combination with CMB shift parameters R , l_a , to place constraints on the DE parameters. Since then more precise data sets have been released. In this work, we present constraints on two metastable DE models using the SNe Ia Pantheon sample (Scolnic et al. 2017), latest BAO data from the 6dF Galaxy Survey (6dFGS) (Beutler et al. 2011), the SDSS DR7 main galaxies sample (MGS) (Ross et al. 2015),

the BOSS DR12 galaxies (Alam et al. 2017a), newly released eBOSS DR14 (Zhao et al. 2018) and high redshift measurement from complete SDSS-III Ly α -quasar cross-correlation function at $z = 2.4$ (Des Bourboux et al. 2017) in combination with CMB distance priors from final full-mission *Planck* measurements of the CMB anisotropies (Aghanim et al. 2018; Chen et al. 2018). The aim of our analysis is to place constraints on metastable DE models using the latest data, compare metastable DE with Λ CDM, and check whether the H_0 tension has been alleviated.

This paper is organized as follows, in section 2 we briefly introduce the Friedmann equations for our model. The observational data to be used including SNe Ia, BAO and distance prior from CMB are presented in section 3. Section 4 contains our main results and some discussion. We summarize our results in section 5.

2. COSMOLOGICAL MODELS

In this work, we test two metastable DE models: (i) in the first DE decays exponentially, (ii) in the second DE decays into non-baryonic dark matter. For comparison, we also place constraints on Λ CDM using the same data sets. We assume that the Friedmann - Lemaitre - Robertson - Walker (FLRW) metric is spatially flat that is strongly supported by recent observations (L’Huillier & Shafieloo 2017; Shafieloo et al. 2018; Aghanim et al. 2018). Under this assumption, the angular diameter distance $D_A(z)$ at redshift z can be written as

$$D_A(z) = \frac{c}{H_0(1+z)} \int_0^z \frac{dz'}{E(z')} \quad (1)$$

where $E(z) = H(z)/H_0$ is the expansion rate and H_0 is the current value of Hubble parameter.

2.1. Λ CDM

Λ CDM model is perhaps the simplest of all dark energy models. In it the cosmological constant Λ plays the role of DE. The Hubble parameter in Λ CDM has the form

$$H^2(z) = H_0^2 [\Omega_{m,0}(1+z)^3 + \Omega_{DE}] \quad (2)$$

where $\Omega_{m,0}$ is the current matter density parameter and $\Omega_{DE} = \frac{\Lambda}{3H_0^2}$ is the density parameter associated with dark energy.

2.2. Model I: Exponentially decaying DE

In this model, DE decays exponentially as

$$\dot{\rho}_{DE} = -\Gamma\rho_{DE} \quad (3)$$

where Γ is the only free parameter in this equation and $\Gamma > 0$ or $\Gamma < 0$ means that DE density is decreasing or increasing, respectively. The Hubble parameter obtained from the FRW equations can be written as

$$H^2(z) = H_0^2 [\Omega_{m,0}(1+z)^3 + (1 - \Omega_{m,0}) \exp\left(\frac{\Gamma}{H_0} \int_0^z \frac{dz'}{E(z')(1+z')}\right)] \quad (4)$$

2.3. Model II: DE decays into DM

In this model dark energy decays into non-baryonic dark matter as follows:

$$\dot{\rho}_{\text{DE}} = -\Gamma \rho_{\text{DE}} \quad (5)$$

$$\dot{\rho}_{\text{DM}} + 3H\rho_{\text{DM}} = \Gamma \rho_{\text{DE}} \quad (6)$$

This model is effectively an interacting DE-DM model since when $\Gamma \neq 0$, energy is exchanged between DM and DE. The Hubble parameter for this model can be written as

$$H^2(z) = H_0^2 [\Omega_{\text{DE}}(z) + \Omega_{\text{DM}}(z) + \Omega_{b,0}(1+z)^3] \quad (7)$$

Here $\Omega_{b,0}$ is the baryon density. Since in this model DE interacts with non-baryonic DM, we need to separate DM density from baryon density. While for metastable DE model I, dark matter and baryon matter can be treated as a whole, e.g., $\Omega_{m,0} = \Omega_{\text{DM},0} + \Omega_{b,0}$.

For the metastable DE models, the cosmological parameters to be constrained are $\{\Omega_{m,0}, H_0, \Gamma\}$. Both model I and model II become Λ CDM when $\Gamma = 0$. We refer the reader to [Shafieloo et al. \(2017\)](#) for more details about these two DE models.

3. DATA AND ANALYSIS

In this work, we consider the combination of three different kinds of cosmological probes to put constraints on DE models, including SNe Ia as standard candles and BAO together with CMB as standard rulers.

3.1. Type Ia Supernovae

In their role as standard candles, SNe Ia have been of great importance to measure cosmological distances. In our analysis, we use the new "Pantheon" sample ([Scolnic et al. 2017](#)), which is the largest combined sample of SN Ia and consists of 1048 data with redshifts in the range $0.01 < z < 2.3$. In order to reduce the impact of calibration systematics on cosmology, the Pantheon compilation used cross-calibration of the photometric systems of all the subsamples used to construct the final sample.

3.2. Baryonic Acoustic Oscillations

The second data set used in our analysis is BAO. It includes lower redshift BAO measurements from galaxy surveys and higher redshift BAO measurement from Lyman- α forest (Ly α) data. For the lower redshift BAO observations, we turn to the latest measurements of acoustic-scale distance ratio from the 6-degree Field Galaxy Survey (6dFGS) ([Beutler et al. 2011](#)), the SDSS Data Release 7 Main Galaxy sample (MGS) ([Ross et al. 2015](#)), the BOSS DR12 galaxies ([Alam et al. 2017a](#)) and the eBOSS DR14 quasars ([Zhao et al. 2018](#)), while the higher redshift BAO measurement is derived from the complete SDSS-III Ly α quasar cross-correlation function at $z = 2.4$ ([Des Bourboux et al. 2017](#)). Details of the BAO measurements are listed in Table 1.

3.3. Cosmic Microwave Background

We include CMB into our analysis by using the CMB distance prior, the acoustic scale l_a and the shift parameter R together with the baryon density $\Omega_b h^2$. The shift parameter is defined as

$$R \equiv \sqrt{\Omega_m H_0^2} r(z_*)/c \quad (8)$$

and the acoustic scale is

$$l_a \equiv \pi r(z_*)/r_s(z_*) \quad (9)$$

where $r(z_*)$ is the comoving distance to the photon-decoupling epoch z_* . We use the distance priors from the finally release *Planck* TT, TE, EE +low E data in 2018 ([Chen et al. 2018](#)), which makes the uncertainties 40% smaller than those from *Planck* TT+low P.

When using SNe Ia and BAO as cosmological probes, we use a conservative prior for $\Omega_b h^2$ based on the measurement of D/H by [Cooke et al. \(2018\)](#) and standard BBN with modelling uncertainties. The constraint results are obtained with Markov Chain Monte Carlo (MCMC) estimation using *CosmoMC* ([Lewis & Bridle 2002](#)).

In our analysis, four kinds of combined data sets are considered: 1) Pantheon compilation in combination with BAO data from 6dFGS, MGS and BOSS DR12. 2) We add BAO data from eBOSS DR14 to the first data set. 3) Adding high redshift BAO measurement from Ly α to the second data combination. 4) Finally, we include the CMB distance prior to the full combination of data sets.

4. RESULTS AND DISCUSSION

We first show the constraints for the Λ CDM model in Fig. 1 where the different colors denote the results from

Table 1. BAO measurements used in our analysis. Here r_d is the comoving sound horizon at the baryon drag epoch z_{drag} , and $D_V = [(1+z)^2 D_A^2(z) cz/H(z)]^{1/3}$, $D_M = (1+z)D_A$, where D_A is the angular diameter distance defined in equation (1). The fiducial comoving sound horizon for BOSS DR12, eBOSS DR14 and Ly α is $r_{d,\text{fid}} = 147.78$ Mpc. In practice, our analysis uses the full covariance matrix for BAO measurements from Alam et al. (2017a); Zhao et al. (2018); Des Bourboux et al. (2017).

z	D_V/r_d	$D_M \times (r_{d,\text{fid}}/r_d)(\text{Mpc})$	$H \times (r_d/r_{d,\text{fid}})(\text{km/s/Mpc})$	$D_A \times (r_{d,\text{fid}}/r_d)(\text{Mpc})$	Ref.
0.106	3.047 ± 0.137	-	-	-	Beutler et al. (2011)
0.150	4.480 ± 0.168	-	-	-	Ross et al. (2015)
0.38	-	1512 ± 24	81.2 ± 2.4	-	Alam et al. (2017a)
0.51	-	1975 ± 30	90.9 ± 2.4	-	
0.61	-	2307 ± 37	99.0 ± 2.5	-	
0.978	-	-	113.72 ± 14.63	1586.18 ± 284.93	Zhao et al. (2018)
1.230	-	-	131.44 ± 12.42	1769.08 ± 159.67	
1.526	-	-	148.11 ± 12.75	1768.77 ± 96.59	
1.944	-	-	172.63 ± 14.79	1586.18 ± 146.46	
2.4	-	5393.4 ± 176.8	227.56 ± 5.6	-	Des Bourboux et al. (2017)

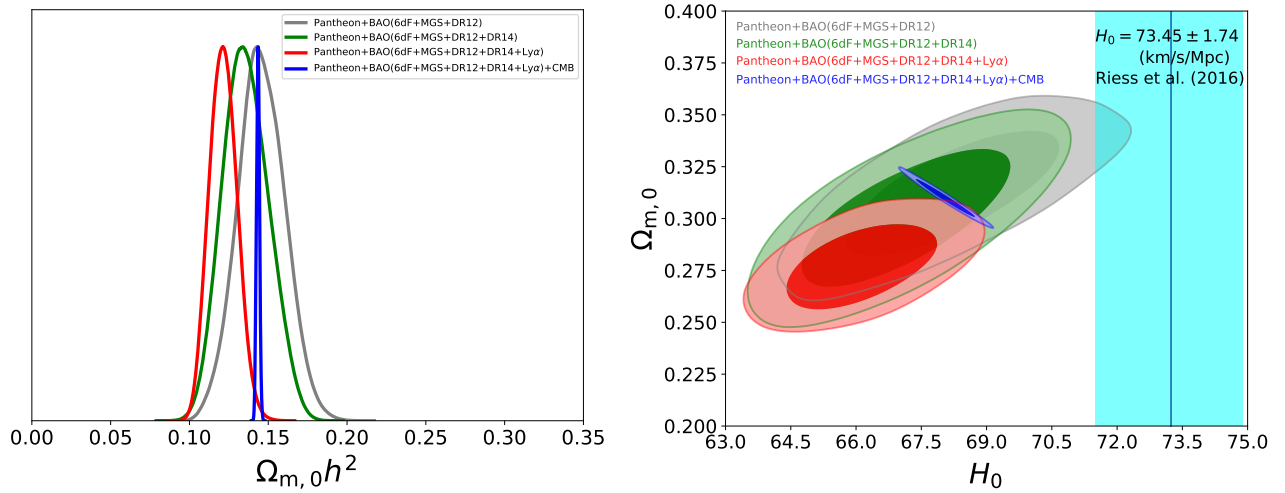


Figure 1. Observed constraints on standard Λ CDM. Left plot gives the 1D likelihood for $\Omega_{m,0}h^2$ and right plots shows the 1σ and 2σ contours for $\Omega_{m,0}$ vs H_0 . The cyan shadow in the right plot give H_0 results from Riess et al. (2016) and we show the constrain results from different data sets in different color.

Table 2. The best fit of cosmological parameters (the first row in each parameter row) for Λ CDM and its mean value together with its marginalized 1σ uncertainties (the second row in each parameter row) as well as their χ^2 value.

data	Pantheon	Pantheon	Pantheon	Pantheon
	+BAO(6dF+MGS+DR12)	+BAO(6dF+MGS+DR12	+BAO(6dF+MGS+DR12	+BAO(6dF+MGS+DR12
parameters		+DR14)	+DR14+Ly α)	+DR14+Ly α)+CMB
$\Omega_{m,0}$	0.312	0.299	0.276	0.310
	$0.313^{+0.020}_{-0.021}$	$0.301^{+0.021}_{-0.020}$	$0.277^{+0.013}_{-0.014}$	$0.310^{+0.006}_{-0.006}$
H_0	68.10	67.03	66.0	68.06
	$68.22^{+1.65}_{-1.69}$	$67.17^{+1.56}_{-1.54}$	$66.08^{+1.19}_{-1.14}$	$68.05^{+0.46}_{-0.43}$
$\Omega_{m,0}h^2$	0.145	0.134	0.1083	0.144
	$0.146^{+0.016}_{-0.015}$	$0.135^{+0.016}_{-0.013}$	$0.121^{+0.009}_{-0.009}$	$0.144^{+0.001}_{-0.001}$
χ^2	1042.58	1046.94	1064.58	1071.14

different data combinations. The left plot shows the 1D marginalized results for $\Omega_{m,0}h^2$ and the right plot

presents the 2D marginalized 1σ and 2σ contours of $\Omega_{m,0}$ vs H_0 . In the right plot, we also show the H_0 constraints from Riess et al. (2016) in the cyan shadow. The best fit for cosmological parameters of Λ CDM and their 1σ uncertainties are summarized in Table 2. We also show the χ^2 from each data combination in Table 2. From Fig. 1 and Table 2, we can clearly see that, adding BAO measurements from eBOSS DR14 pushes the best fit of $\Omega_{m,0}$ and H_0 towards a lower value (the green curves), and including BAO measurement from Ly α makes the best fit of $\Omega_{m,0}$ and H_0 even lower (the red curves). However, a higher matter density and a higher Hubble constant are obtained when using the combined data of Pantheon+BAO(6dF+MGS+DR12+DR14+Ly α)+CMB (the blue curves), which makes the best fits of $\Omega_{m,0}h^2$ in excellent agreement with the results from Pantheon+BAO(6dF+MGS+DR12). One might note that there is a clear tension between the results obtained from adding high redshift Ly α BAO measurement and the results obtained from including CMB. We should note that this tension has been reported earlier by Sahni et al. (2014); Shafieloo et al. (2017). It is important to emphasize here that one of our main aims is to see whether we can alleviate this tension by analyzing the metastable DE models using current data sets.

In Fig. 2 we show the results for the metastable DE model I, in which DE decays exponentially. We show the 1D likelihoods for $\Omega_{m,0}h^2$ and Γ/H_0 in the upper plots and the 2D marginalized 1σ and 2σ contours in the lower plots. As before, different colors imply different data combinations. The two left plots should be compared with Fig. 1. The best fit for the cosmological parameters of model I and the marginalized 1σ uncertainties as well as the χ^2 of each data combination are presented in Table 3. Compared with Λ CDM, the confidence contours are much larger. However, the H_0 tension between higher redshift BAO measurements from Ly α and CMB increases. Lower matter density and lower Hubble parameter are favoured by adding high redshift BAO measurements from Ly α .

Moreover, from the two right plots of Fig. 2 we can see that the constraint on Γ/H_0 obtained with Pantheon+BAO(6dF+MGS+DR12) (grey curves) support $\Gamma < 0$ while the results obtained with Pantheon+BAO(6dF+MGS+DR12+DR14) (green curves) support either $\Gamma < 0$ or $\Gamma > 0$, which means that Pantheon+BAO(6dF+MGS+DR12) data suggest that the DE density is increasing, while for Pantheon in combination with BAO(6dF+MGS+DR12+DR14) the best fits on Γ don't show any preference for the DE density to be either increasing or decreasing. However, adding Ly α

BAO data into the analysis gives $\Gamma > 0$ (red curves), which means DE density decays with time, in other words the DE density at earlier times was larger than at present. On the other hand, results obtained after including the CMB distance prior lie close to $\Gamma = 0$ (blue curves) suggesting that Λ CDM is preferred by the CMB data set. This might be due to the fact that CMB distance priors are obtained assuming Λ CDM cosmology.

In Fig. 3, Fig. 4, Fig. 5 and Fig. 6, we show the Hubble parameter as a function of redshift $H(z)$, the equation of state of dark energy as a function of redshift $w(z)$, the Om diagnostic $Om(z) = (h^2(z) - 1)/[(1+z)^3 - 1]$ and the deceleration parameter $q(z) = -\ddot{H}/H^2 - 1$ for the metastable DE model I. We plot 100 samples for these parameters randomly chosen from within 2σ range of the MCMC chains corresponding to different data sets.

Fig. 7 shows the corresponding results for the metastable DE model II. The upper two plots show the 1D likelihoods for $\Omega_{m,0}h^2$ (left) and Γ/H_0 (right) obtained from different data combinations. The lower plots show the 2D marginalized 1σ and 2σ regions for $\Omega_{m,0}$ vs H_0 (left plot) and Ω_{DE} vs Γ/H_0 (right plot). The details of the best fits and 1σ uncertainties for parameters of model II are summarized in Table 4. From the left bottom plot and Table 4, we can see that adding BAO measurement from Ly α makes the best fit of $\Omega_{m,0}$ larger than it obtained without BAO measurement from Ly α . While the constrain results for H_0 become lower when including BAO measurement from Ly α . However, adding CMB distance prior to the data set pushes the results back to higher H_0 and lower $\Omega_{m,0}$. The H_0 tension still exists between CMB and BAO measurement from Ly α . However, as can be seen from the upper left plot, $\Omega_{m,0}h^2$ agrees well between CMB and BAO measurement from Ly α since the degeneracy of contours for $\Omega_{m,0}$ and H_0 changes.

Now let's look at the two right plots, which focus on the constraints on Γ from observations. As mentioned earlier, $\Gamma > 0$ implies that DE decays into dark matter, while $\Gamma < 0$ means the opposite: dark matter decays into DE. Our model becomes Λ CDM when $\Gamma = 0$. We find that, with Pantheon in combination with BAO data from 6dFGS, MGS and BOSS DR12, the best fit for Γ supports the transfer of energy from dark matter to dark energy, while adding BAO measurements from eBOSS DR14 and Ly α favours the opposite. Including CMB distance prior to the analysis gives $\Gamma \simeq 0$, which means that the DE energy density remains unchanged.

In Fig. 8, Fig. 9 and Fig. 10, we also show the Hubble parameter as a function of redshift $H(z)$, the Om diag-

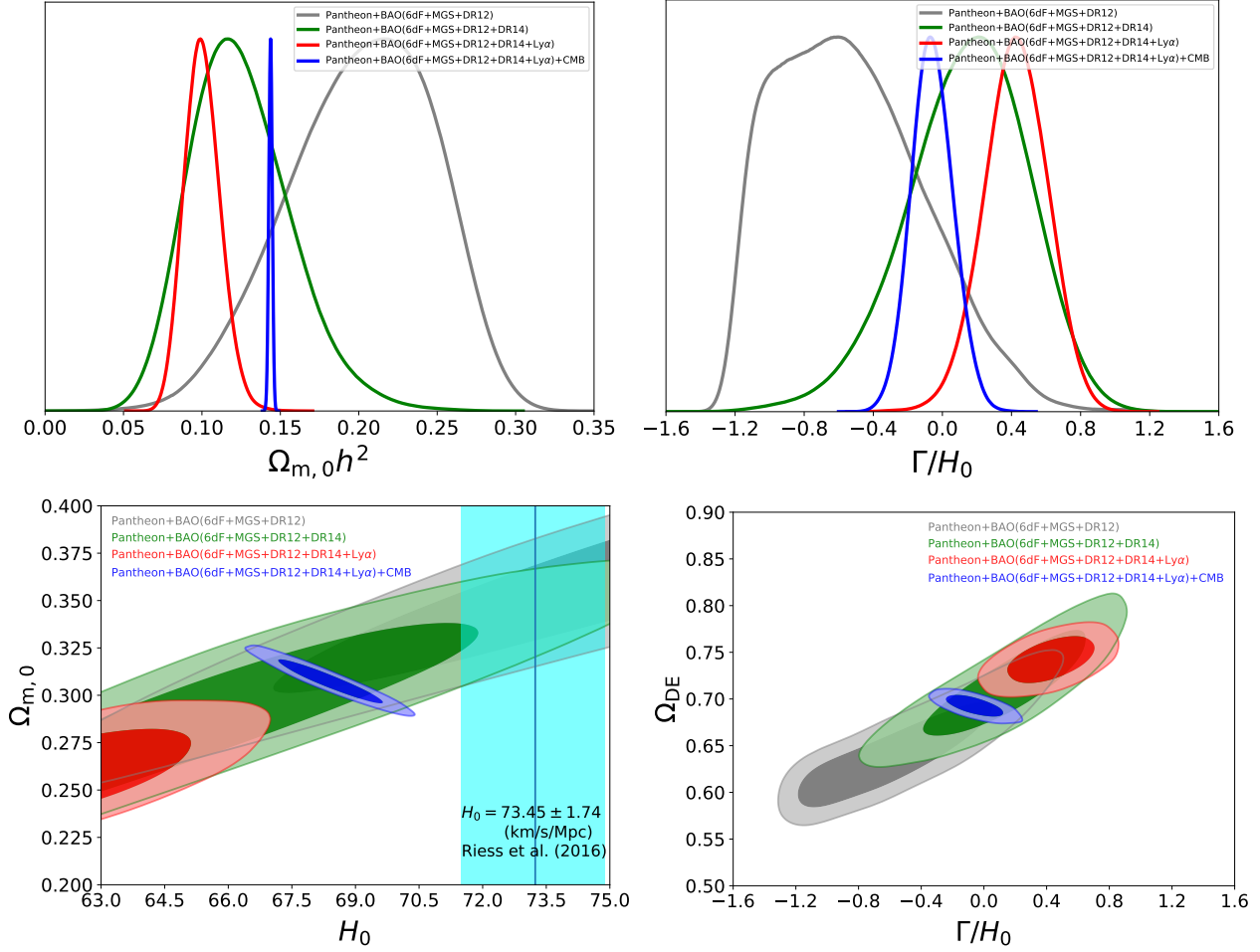


Figure 2. Observed constraints on model I. The upper two plots show the marginalized 1D likelihood for $\Omega_{m,0}h^2$ (left) and Γ/H_0 (right). The lower two plots show the marginalized 1σ and 2σ contours for matter density vs Hubble constant (left) and Ω_{DE} vs Γ/H_0 (right). Different color denotes for the constraint results from different data sets.

Table 3. The best fit of cosmological parameters (the first row in each parameter row) for the metastable DE model I and its mean value together with its marginalized 1σ uncertainties (the second row in each parameter row) as well as their χ^2 value.

data	Pantheon +BAO(6dF+MGS+DR12)	Pantheon +BAO(6dF+MGS+DR12 +DR14)	Pantheon +BAO(6dF+MGS+DR12 +DR14+Ly α)	Pantheon +BAO(6dF+MGS+DR12 +DR14+Ly α)+CMB
$\Omega_{m,0}$	0.360 $0.360^{+0.033}_{-0.042}$	0.276 $0.288^{+0.037}_{-0.38}$	0.256 $0.259^{+0.017}_{-0.016}$	0.307 $0.307^{+0.008}_{-0.008}$
H_0	75.09 $75.01^{+4.71}_{-5.80}$	64.03 $65.53^{+4.60}_{-4.41}$	61.98 $62.29^{+1.99}_{-1.94}$	68.45 $68.38^{+0.83}_{-0.82}$
$\Omega_{m,0}h^2$	0.203 $0.203^{+0.046}_{-0.050}$	0.113 $0.124^{+0.036}_{-0.030}$	0.098 $0.100^{+0.0124}_{-0.190}$	0.144 $0.144^{+0.001}_{-0.001}$
Γ/H_0	-0.57 $-0.55^{+0.46}_{-0.40}$	0.25 $0.14^{+0.34}_{-0.37}$	0.45 $0.42^{+0.19}_{-0.19}$	-0.06 $-0.06^{+0.13}_{-0.12}$
χ^2	1041.52	1046.42	1058.94	1070.94

nostic $Om(z) = (h^2(z)-1)/[(1+z)^3-1]$ and the deceleration parameter $q(z) = -\ddot{H}/H^2 - 1$ for the metastable

DE model II, respectively. We plot 100 samples for these

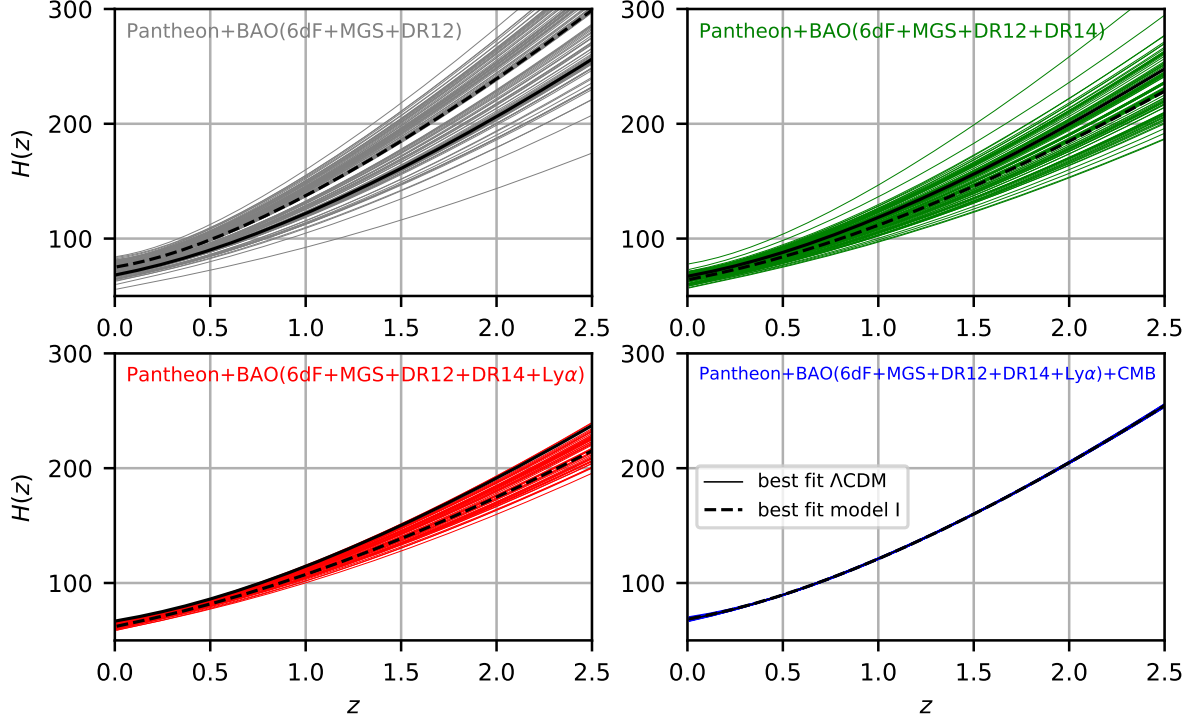


Figure 3. The Hubble parameter $H(z)$ for the metastable DE model I obtained with different data combinations. The solid black lines and the dashed black lines show $H(z)$ from the best fit of the Λ CDM model and the metastable DE model I with same data set, respectively.

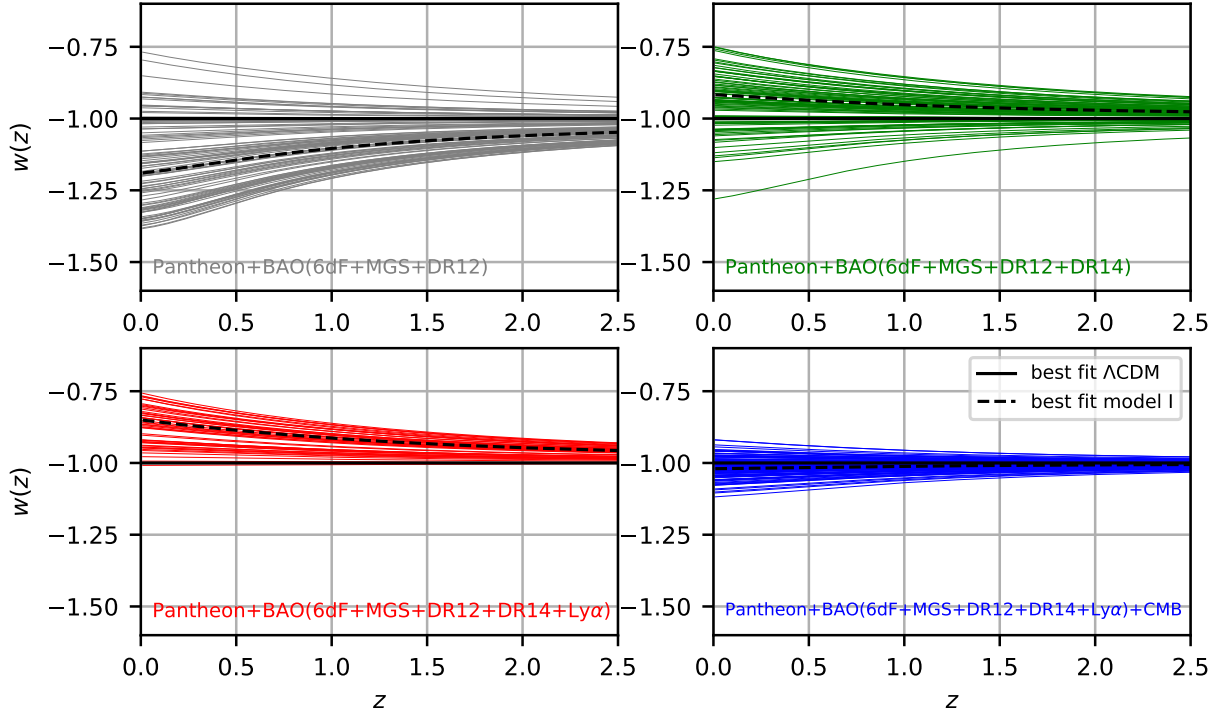


Figure 4. The equation of state of dark energy as a function of redshift for the metastable DE model I obtained with different data combinations. The solid black lines and the dashed black lines show $w(z)$ from the best fit of the Λ CDM model and the metastable DE model I with same data set, respectively.

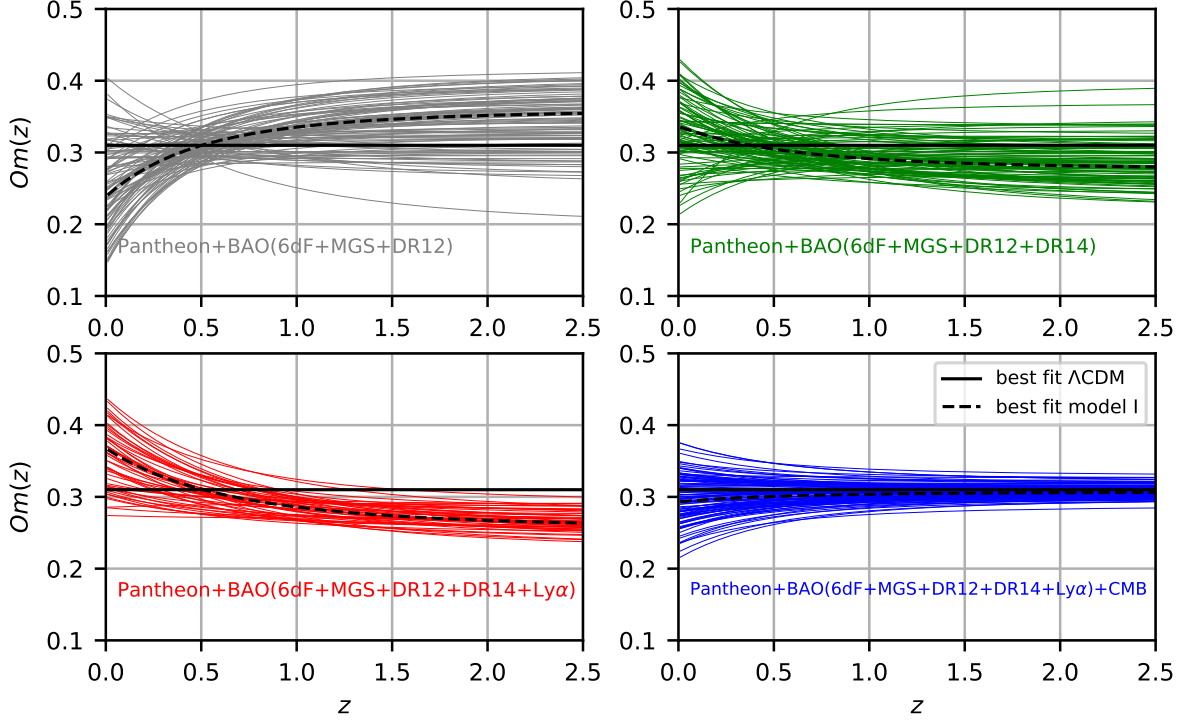


Figure 5. The Om diagnostic as a function of redshift for the metastable DE model I obtained with different data combinations. The solid black lines and the dashed black lines show $Om(z)$ from the best fit of the Λ CDM model and the metastable DE model I with the same data set, respectively.

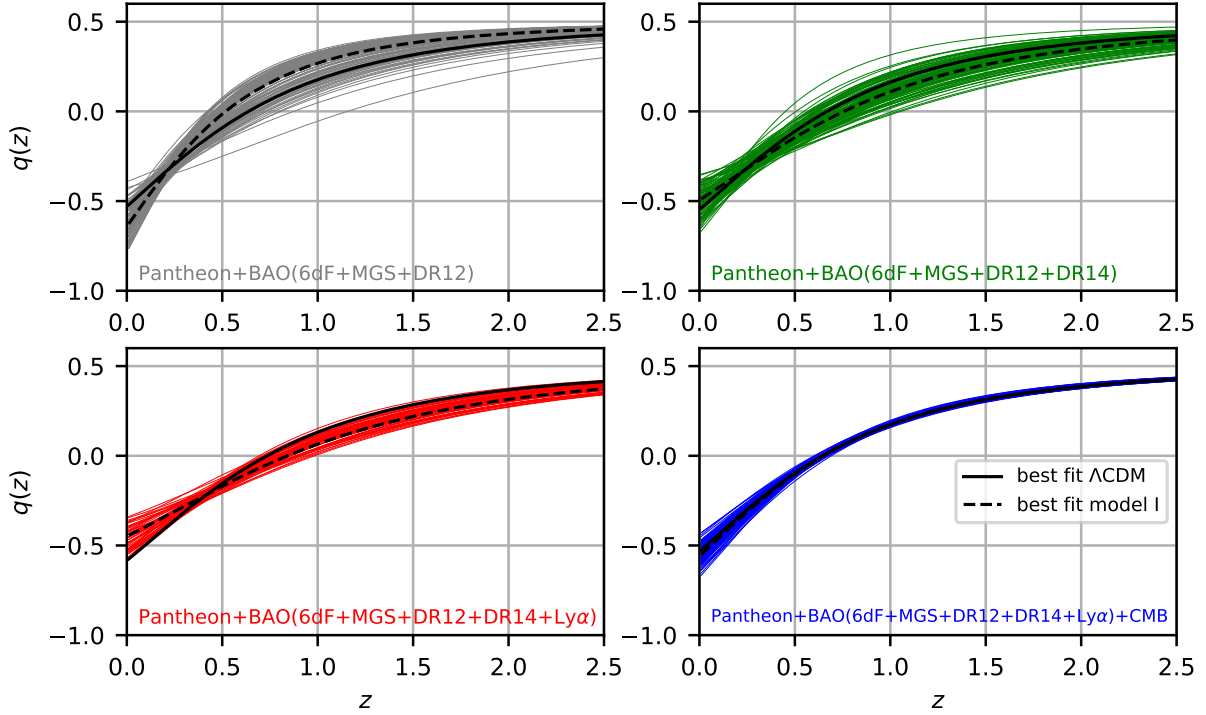


Figure 6. The deceleration parameter as a function of redshift for the metastable DE model I obtained with different data combinations. The solid black lines and the dashed black lines show $q(z)$ from the best fit of the Λ CDM model and the metastable DE model I with the same data set, respectively.

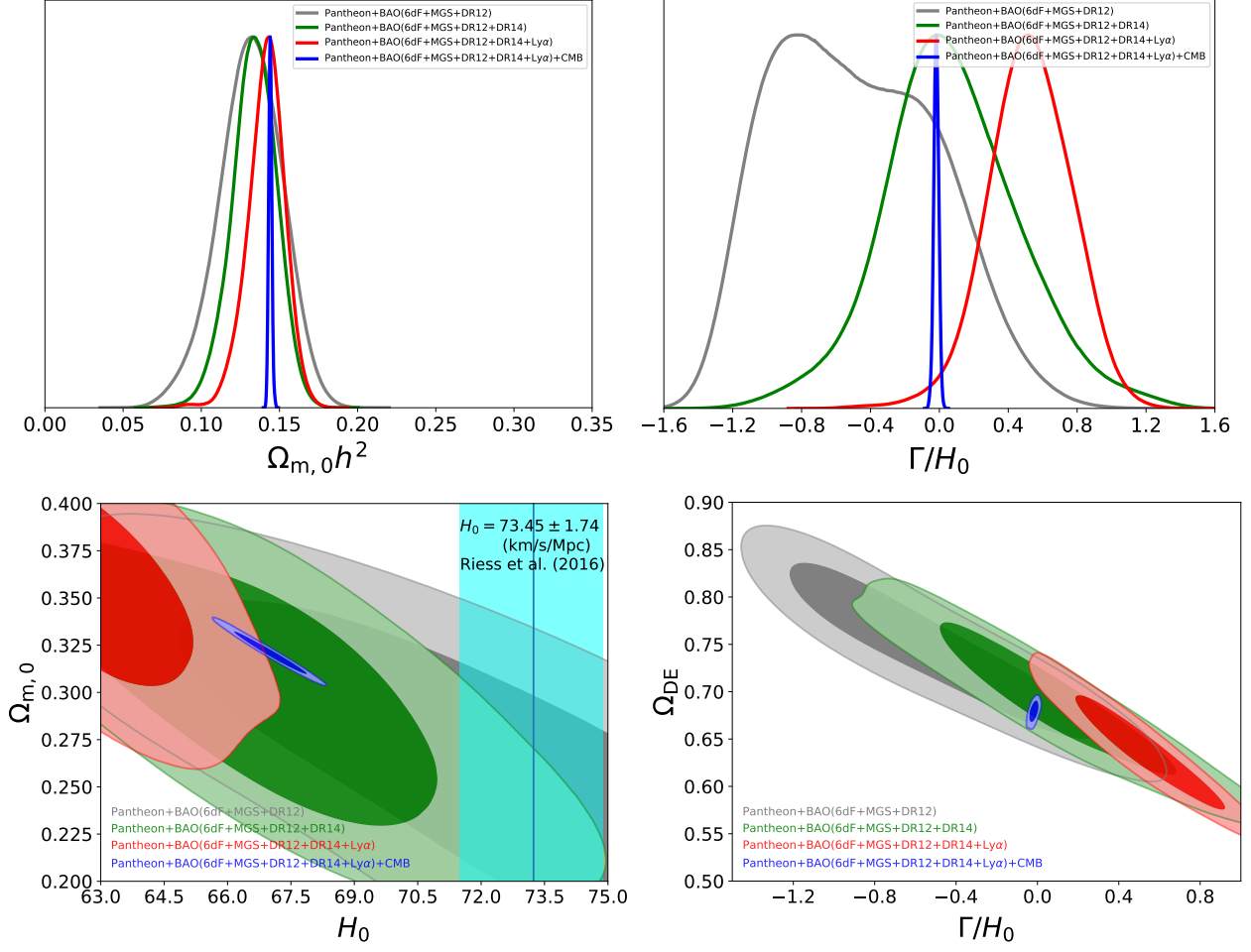


Figure 7. The constrain results for Model II. The upper two plots show the marginalized 1D likelihood for $\Omega_{m,0}h^2$ (left) and Γ/H_0 (right). The lower two plots show the marginalized 1σ and 2σ regions for matter density vs Hubble constant (left) and Ω_{DE} vs Γ/H_0 (right). Different color denotes for the constraint results from different data sets.

Table 4. The best fit of cosmological parameters (the first row in each parameter row) and its mean value together with its marginalized 1σ uncertainties (the second row in each parameter row) for metastable DE model II obtained from different data combination. The last row show the χ^2 value of each data combination.

data	Pantheon +BAO(6dF+MGS+DR12)	Pantheon +BAO(6dF+MGS+DR12 +DR14)	Pantheon +BAO(6dF+MGS+DR12 +DR14+Ly α)	Pantheon +BAO(6dF+MGS+DR12 +DR14+Ly α)+CMB
$\Omega_{m,0}$	0.253 0.263 $^{+0.056}_{-0.060}$	0.314 0.304 $^{+0.048}_{-0.048}$	0.367 0.362 $^{+0.042}_{-0.043}$	0.319 0.321 $^{+0.008}_{-0.007}$
H_0	72.61 71.80 $^{+4.71}_{-4.58}$	66.74 66.94 $^{+2.55}_{-3.43}$	62.30 62.64 $^{+1.85}_{-1.70}$	67.11 66.98 $^{+0.56}_{-0.57}$
$\Omega_{m,0}h^2$	0.133 0.134 $^{+0.019}_{-0.021}$	0.137 0.136 $^{+0.014}_{-0.014}$	0.142 0.142 $^{+0.012}_{-0.013}$	0.144 0.144 $^{+0.001}_{-0.001}$
Γ/H_0	-0.78 -0.47 $^{+0.50}_{-0.50}$	0.03 0.07 $^{+0.40}_{-0.30}$	0.57 0.51 $^{+0.27}_{-0.25}$	-0.01 -0.02 $^{+0.01}_{-0.01}$
χ^2	1041.55	1046.50	1059.08	1071.03

parameters randomly chosen from within 2σ range of the MCMC chains corresponding to different data sets.

In Fig. 11, we show the $H(z)$ samples within 2σ confidence level for different cosmological models obtained

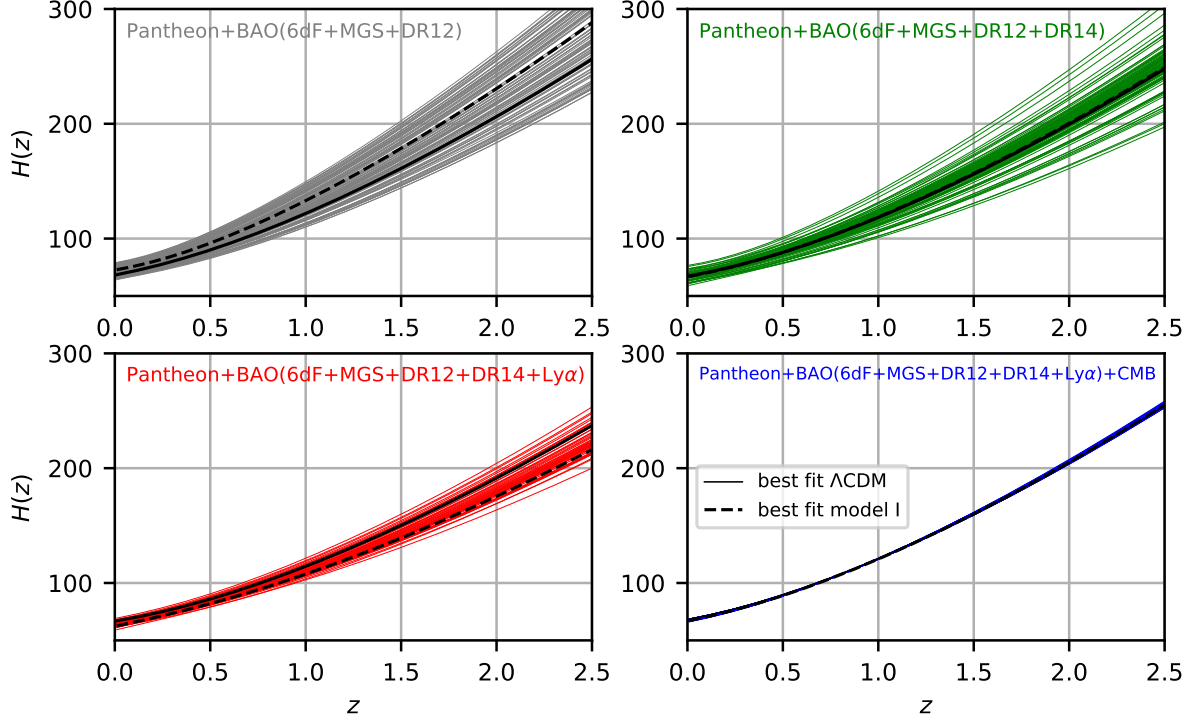


Figure 8. The Hubble parameter $H(z)$ for the metastable DE model II obtained with different data combinations. The solid black lines and the dashed black lines show $H(z)$ from the best fit of the Λ CDM model and the metastable DE model II with the same data set, respectively.

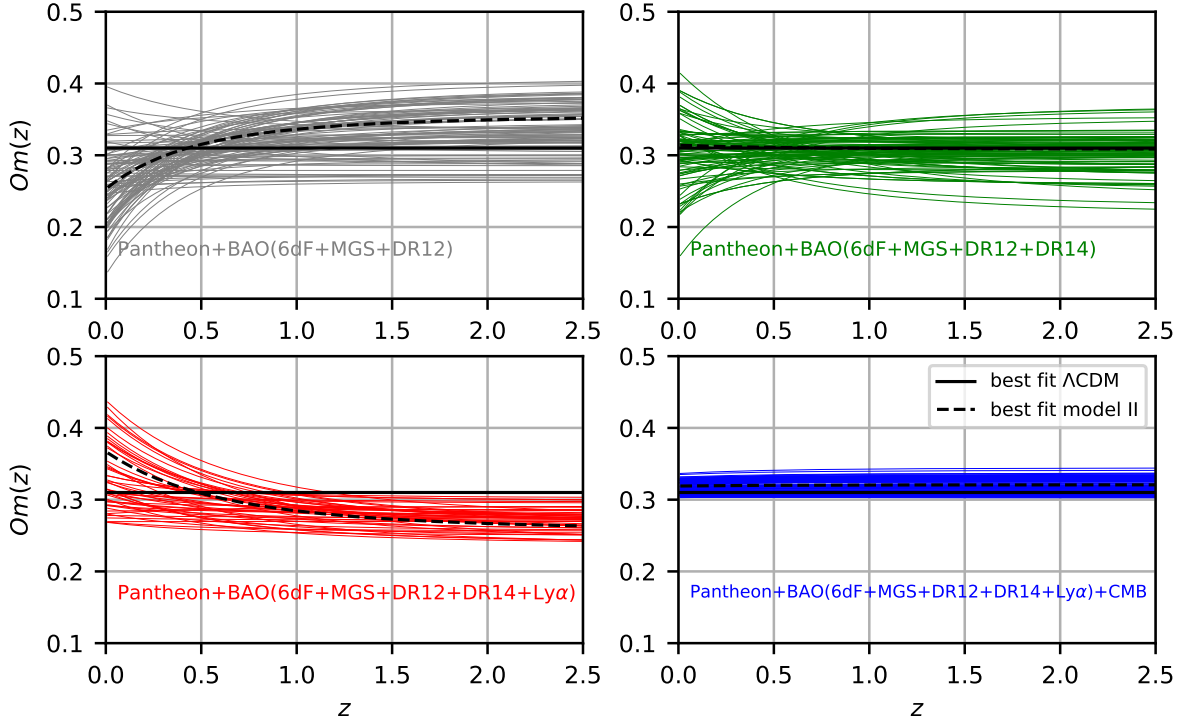


Figure 9. The Om diagnostic as a function of redshift for the metastable DE model II obtained with different data combinations. The solid black lines and the dashed black lines show $Om(z)$ from the best fit of the Λ CDM model and the metastable DE model II with the same data set, respectively.

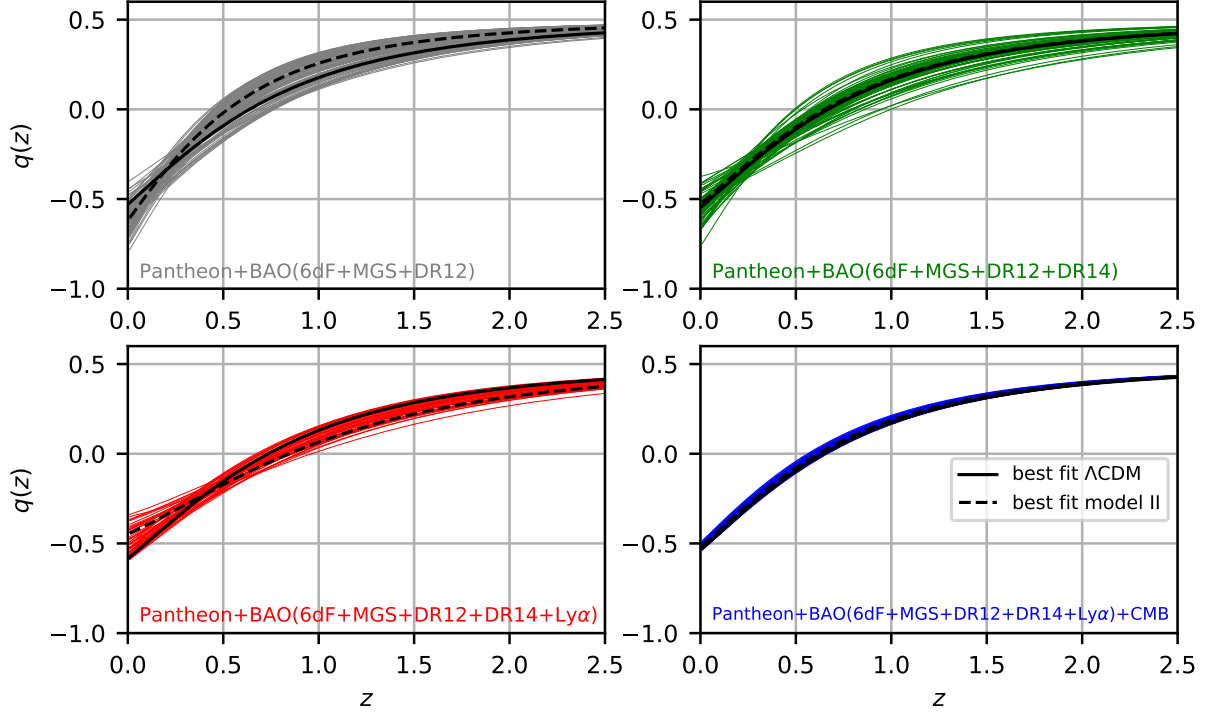


Figure 10. The deceleration parameter as a function of redshift for the metastable DE model II obtained with different data combinations. The solid black lines and the dashed black lines show $q(z)$ from the best fit of the Λ CDM model and the metastable DE model II with the same data set, respectively.

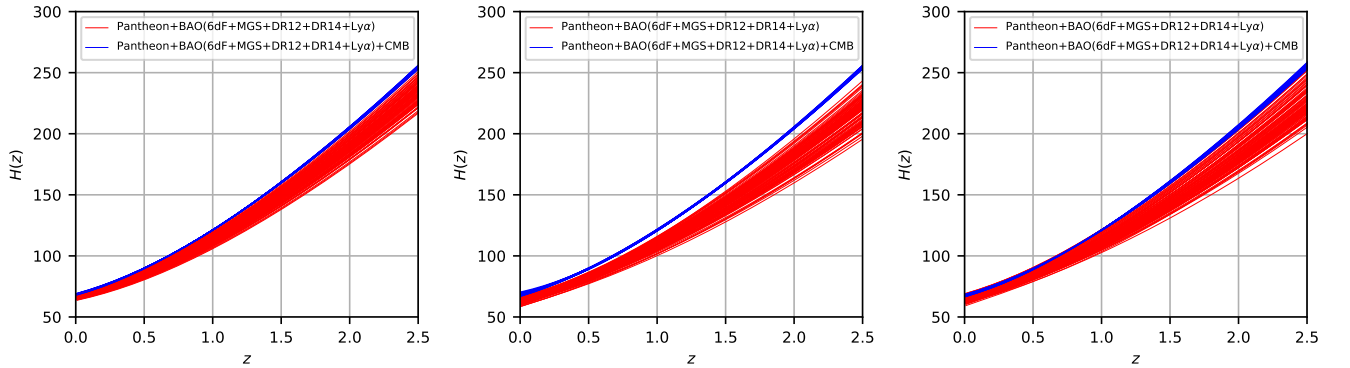


Figure 11. Hubble parameter for different cosmological models constrained with two different data sets described above. From left to right, we show Hubble parameter as a function of redshift for standard Λ CDM model, metastable model I and model II, respectively.

with different data combinations including SNe Ia, BAO and CMB. The left plot shows the Λ CDM model results which shows that for the data set combination with and without CMB data the sample shows little overlap. While for the metastable DE model I, which is shown in the middle plot of Fig. 11, there is apparently no overlap. The results for the metastable DE model II are shown in the right plot of Fig. 11, which is similar to Λ CDM.

Using current data sets of SNe Ia, BAO and CMB, we find that the H_0 tension between CMB and BAO measurements from Ly α existing in Λ CDM model (see Fig. 1) become larger when compared with the results obtained from previous data sets (see Fig. 1 in Shafieloo et al. (2017)) and metastable DE models cannot reduce this H_0 tension. Including the CMB distance prior to our analysis shows that both model I and model II are consistent with Λ CDM model, while without CMB data, the results from Pantheon in combination with BAO(6dF+MGS+DR12+DR14+Ly α) support that DE density is decaying (exponentially for the model I and into dark matter density for the model II).

5. SUMMARY

In this work, we revisit two metastable DE models proposed in Shafieloo et al. (2017) confronting them with the Pantheon SNe Ia sample, BAO measurements derived from 6dFGS, the SDSS DR7 MGS sample, the BOSS DR12, the eBOSS DR14 and high redshift BAO measurement from the Ly α forest in combination with the CMB distance prior from the final *Planck* release in 2018.

In the metastable DE models, the DE density decays exponentially in the model I and decays into dark matter in the model II (the reverse process DM \rightarrow DE is also permitted). The specific feature of these two models is that the decay rate is a constant and depends only on intrinsic properties of dark energy and not on other factors such as cosmological expansion, etc.

We estimate some key cosmological parameters assuming standard Λ CDM on the one hand, and the two metastable DE models on the other. We find that with current data sets, the $\Omega_{0m}h^2$ tension between CMB and high redshift BAO measurement from Ly α becomes significant in Λ CDM and also in the model I. The model II shows slightly better consistency. We should note that the degeneracy direction for $\Omega_{m,0}$ vs H_0 for the model II is different from the model I, that makes constraints on the derived parameter $\Omega_{m,0}h^2$ to agree better with CMB and high redshift BAO measurements. Marginalised probability distribution function for H_0 in the metastable dark energy models including super-

novae and all BAO data (except the Ly α BAO data) shows clear consistency with the results including Planck CMB constraints. However, including Ly α BAO data (and without Planck CMB measurements) changes the constraints on H_0 dramatically, lowering it to a central value of 62 km/sec/Mpc. Since local measurements of the Hubble constant place its value to be around 73 km/sec/Mpc, the situation seems to be very conflicting. In fact Ly α BAO data, Planck CMB data and the local measurement of H_0 , each pull our models to a different region in parameter space. This could be due to tension between different data sets. Possible resolutions of this dilemma might lie in systematics in some of the data, a more complicated form of the expansion history (which needs to be reconstructed carefully to satisfy all observations) or an unconventional model of the early Universe (Hazra et al. 2019).

We should note here that from a statistical point of view and to compare the analysed metastable dark energy models in this paper with Λ CDM model, we do not expect that these models perform better than the standard Λ CDM model by estimating the Bayes factor (as done in Pan et al. (2019), analysing the model proposed in Li & Shafieloo (2019)). The fact is that having an extra degree of freedom in these metastable models, we have not achieved a substantial improvements in the likelihood estimations (as shown in Table 2, 3, 4). In such a situation, the Bayesian analysis prefers a model with lower degrees of freedom (Λ CDM model). However, future data with higher precision and better control of systematics might change the current situation and we might get substantially different likelihoods for these models in comparison to the standard Λ CDM model. This might not be surprising as the standard Λ CDM model has problems fitting the low and high redshift data simultaneously, and with higher precision data the likelihood for this model might get substantially worsen. This is the main reason why we should continue to study models that might not be currently favoured compared to the standard model while they may have interesting phenomenological or theoretical properties.

By the time we were finalising our work, a recent work by Riess et al. (2019) came out and in their work they showed a larger H_0 tension between locally measurement and the value inferred from *Planck* CMB and Λ CDM. It is therefore extremely important to understand the nature of these tensions.

X. Li thanks Ryan E. Keeley and Benjamin L’Huillier for valuable suggestions. X. Li thanks Jingzhao Qi for kindly instructions about *Cosmomc*. X. Li and A.S. would like to acknowledge the support of

the National Research Foundation of Korea (NRF-2016R1C1B2016478). X. Li was supported by the fund of Hebei Normal University. X. Li was supported by the Strategic Priority Research Program of the Chinese Academy of Sciences, Grant No. XDB23000000. A.A.S.

was partly supported by the program KP19-270 "Questions of the origin and evolution of the Universe" of the Presidium of the Russian Academy of Sciences. This work benefits from the high performance computing clusters Polaris and Seondeok at the Korea Astronomy and Space Science Institute.

REFERENCES

- Abazajian, K., Adelman-McCarthy, J. K., Agüeros, M. A., et al. 2004, *The Astronomical Journal*, 128, 502
- Ade, P. A., Aghanim, N., Arnaud, M., et al. 2016, *Astronomy & Astrophysics*, 594, A13
- Aghanim, N., Akrami, Y., Ashdown, M., et al. 2018, arXiv preprint arXiv:1807.06209
- Alam, S., Ata, M., Bailey, S., et al. 2017a, *Monthly Notices of the Royal Astronomical Society*, 470, 2617
- Alam, U., Bag, S., & Sahni, V. 2017b, *Physical Review D*, 95, 023524
- Bean, R., Carroll, S., & Trodden, M. 2005, arXiv preprint astro-ph/0510059
- Beutler, F., Blake, C., Colless, M., et al. 2011, *Monthly Notices of the Royal Astronomical Society*, 416, 3017
- Cao, S., Biesiada, M., Gavazzi, R., Piórkowska, A., & Zhu, Z.-H. 2015, *The Astrophysical Journal*, 806, 185
- Chen, L., Huang, Q.-G., & Wang, K. 2018, arXiv preprint arXiv:1808.05724
- Collaboration, P., Ade, P., Aghanim, N., Armitage-Caplan, C., et al. 2014, *Astron. Astrophys*, 571, A16
- Cooke, R. J., Pettini, M., & Steidel, C. C. 2018, *The Astrophysical Journal*, 855, 102
- Des Bourboux, H. D. M., Le Goff, J.-M., Blomqvist, M., et al. 2017, *Astronomy & Astrophysics*, 608, A130
- Di Valentino, E., Linder, E. V., & Melchiorri, A. 2018, *Physical Review D*, 97, 043528
- Di Valentino, E., Melchiorri, A., & Mena, O. 2017, *Physical Review D*, 96, 043503
- Ding, X., Biesiada, M., Cao, S., Li, Z., & Zhu, Z.-H. 2015, *The Astrophysical Journal Letters*, 803, L22
- Eisenstein, D. J., Zehavi, I., Hogg, D. W., et al. 2005, *The Astrophysical Journal*, 633, 560
- Hazra, D. K., Shafieloo, A., & Souradeep, T. 2019, *Journal of Cosmology and Astroparticle Physics*, 2019, 036
- Khosravi, N., Baghran, S., Afshordi, N., & Altamirano, N. 2019, *Physical Review D*, 99, 103526
- Ko, P., Nagata, N., & Tang, Y. 2017, *Physics Letters B*, 773, 513
- Komatsu, E., Dunkley, J., Nolte, M., et al. 2009, *The Astrophysical Journal Supplement Series*, 180, 330
- Kumar, S., & Nunes, R. C. 2017, *Physical Review D*, 96, 103511
- Lewis, A., & Bridle, S. 2002, *Physical Review D*, 66, 103511
- L’Huillier, B., & Shafieloo, A. 2017, *Journal of Cosmology and Astroparticle Physics*, 2017, 015
- Li, X., Cao, S., Zheng, X., et al. 2017, *The European Physical Journal C*, 77, 677
- Li, X., & Shafieloo, A. 2019, *The Astrophysical Journal Letters*, 883
- Li, X.-L., Cao, S., Zheng, X.-G., Li, S., & Biesiada, M. 2016, *Research in Astronomy and Astrophysics*, 16, 084
- Pan, S., Yang, W., Di Valentino, E., Shafieloo, A., & Chakraborty, S. 2019, arXiv preprint arXiv:1907.12551
- Perlmutter, S., Aldering, G., Goldhaber, G., et al. 1999, *The Astrophysical Journal*, 517, 565
- Poulin, V., Smith, T. L., Karwal, T., & Kamionkowski, M. 2019, *Physical Review Letters*, 122, 221301
- Raveri, M., Hu, W., Hoffman, T., & Wang, L.-T. 2017, *Physical Review D*, 96, 103501
- Renk, J., Zumalacárregui, M., Montanari, F., & Barreira, A. 2017, *Journal of Cosmology and Astroparticle Physics*, 2017, 020
- Riess, A. G., Casertano, S., Yuan, W., Macri, L. M., & Scolnic, D. 2019, arXiv preprint arXiv:1903.07603
- Riess, A. G., Filippenko, A. V., Challis, P., et al. 1998, *The Astronomical Journal*, 116, 1009
- Riess, A. G., Macri, L. M., Hoffmann, S. L., et al. 2016, *The Astrophysical Journal*, 826, 56
- Ross, A. J., Samushia, L., Howlett, C., et al. 2015, *Monthly Notices of the Royal Astronomical Society*, 449, 835
- Sahni, V., Shafieloo, A., & Starobinsky, A. A. 2014, *The Astrophysical Journal Letters*, 793, L40
- Sahni, V., & Starobinsky, A. 2000, *International Journal of Modern Physics D*, 9, 373
- Scolnic, D., Jones, D., Rest, A., et al. 2017, arXiv preprint arXiv:1710.00845
- Shafieloo, A., Hazra, D. K., Sahni, V., & Starobinsky, A. A. 2017, *Monthly Notices of the Royal Astronomical Society*, 473, 2760
- Shafieloo, A., L’Huillier, B., & Starobinsky, A. A. 2018, *Physical Review D*, 98, 083526
- Shanks, T., Hogarth, L., & Metcalfe, N. 2018, arXiv preprint arXiv:1810.02595

- Solà, J., Gómez-Valent, A., & de Cruz Pérez, J. 2017, *Physics Letters B*, 774, 317
- Spergel, D. N., Verde, L., Peiris, H. V., et al. 2003, *The Astrophysical Journal Supplement Series*, 148, 175
- Suzuki, N., Rubin, D., Lidman, C., et al. 2012, *The Astrophysical Journal*, 746, 85
- Szydlowski, M., Stachowski, A., & Urbanowski, K. 2017, *The European Physical Journal C*, 77, 902
- . 2018, arXiv preprint arXiv: 1812.00616
- Tegmark, M., Strauss, M. A., Blanton, M. R., et al. 2004, *Physical Review D*, 69, 103501
- Vattis, K., Koushiappas, S. M., & Loeb, A. 2019, *Physical Review D*, 99, 121302
- Zhao, G.-B., Raveri, M., Pogosian, L., et al. 2017, *Nature Astronomy*, 1, 627
- Zhao, G.-B., Wang, Y., Saito, S., et al. 2018, arXiv preprint arXiv:1801.03043
- Zheng, X., Biesiada, M., Cao, S., Qi, J., & Zhu, Z.-H. 2017, *Journal of Cosmology and Astroparticle Physics*, 2017, 030
- Zheng, X., Ding, X., Biesiada, M., Cao, S., & Zhu, Z.-H. 2016, *The Astrophysical Journal*, 825, 17